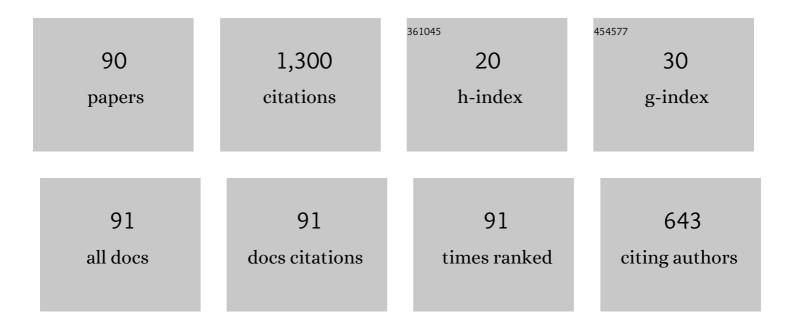
List of Publications by Year in descending order

Source: https://exaly.com/author-pdf/7390281/publications.pdf Version: 2024-02-01



DENC SONC

#	Article	IF	CITATIONS
1	Potential thermal barrier coating materials: <scp>RE</scp> ₃ NbO ₇ (<scp>RE</scp> =La,ÂNd, Sm, Eu, Gd, Dy) ceramics. Journal of the American Ceramic Society, 2018, 101, 4503-4508.	1.9	66
2	Effect of oxygen content in NiCoCrAlY bondcoat on the lifetimes of EB-PVD and APS thermal barrier coatings. Surface and Coatings Technology, 2013, 221, 207-213.	2.2	63
3	Recent progress in thermal/environmental barrier coatings and their corrosion resistance. Rare Metals, 2020, 39, 498-512.	3.6	58
4	Influence of ZrO2 alloying effect on the thermophysical properties of fluorite-type Eu3TaO7 ceramics. Scripta Materialia, 2018, 152, 117-121.	2.6	47
5	Investigation of mechanical and thermal properties of rare earth pyrochlore oxides by firstâ€principles calculations. Journal of the American Ceramic Society, 2019, 102, 2830-2840.	1.9	45
6	Alumina growth behaviour on the surface-modified NiCoCrAl alloy by Pt and Hf at high temperature. Applied Surface Science, 2019, 479, 1178-1191.	3.1	38
7	Oxidation behaviour of the nickel-based superalloy DZ125 hot-dipped with Al coatings doped by Si. Corrosion Science, 2016, 112, 170-179.	3.0	37
8	Alternant phase distribution and wear mechanical properties of an Al 2 O 3 -40 wt%TiO 2 composite coating. Ceramics International, 2017, 43, 7295-7304.	2.3	35
9	Effect of Titanium Addition on Alumina Growth Mechanism on Yttria-Containing FeCrAl-Base Alloy. Oxidation of Metals, 2018, 90, 671-690.	1.0	35
10	Fracture behaviour of ceramic–metallic glass gradient transition coating. Ceramics International, 2019, 45, 5566-5576.	2.3	35
11	Thermo-mechanical properties of fluorite Yb3TaO7 and Yb3NbO7 ceramics with glass-like thermal conductivity. Journal of Alloys and Compounds, 2019, 788, 1231-1239.	2.8	34
12	Influence of the combined-effect of NaCl and Na2SO4 on the hot corrosion behaviour of aluminide coating on Ni-based alloys. Journal of Alloys and Compounds, 2019, 790, 228-239.	2.8	33
13	Effect of exposure conditions on the oxidation of MCrAlY-bondcoats and lifetime of thermal barrier coatings. Surface and Coatings Technology, 2009, 204, 820-823.	2.2	31
14	Effects of the metal-ceramic transition region on the mechanical properties and crack propagation behavior of an Al2O3-40 wt% TiO2 coating. Surface and Coatings Technology, 2017, 321, 200-212.	2.2	30
15	Evolution of cracks within an Al2O3–40 wt%TiO2/NiCoCrAl gradient coating. Ceramics International, 2018, 44, 20798-20807.	2.3	30
16	Microstructure and fracture toughness of in-situ nanocomposite coating by thermal spraying of Ti3AlC2/Cu powder. Ceramics International, 2019, 45, 13119-13126.	2.3	27
17	Microstructure and oxidation behaviour of MoSi2 coating combined MoB diffusion barrier layer on Mo substrate at 1300°C. Ceramics International, 2021, 47, 10137-10146.	2.3	27
18	Microstructure and wear performance of arc-sprayed Al/316L stainless-steel composite coating. Surface and Coatings Technology, 2019, 374, 189-200.	2.2	26

#	Article	IF	CITATIONS
19	Plastic metallic-barrier layer for crack propagation within plasma-sprayed Cu/ceramic coatings. Surface and Coatings Technology, 2019, 360, 259-268.	2.2	24
20	Thermal properties of Y1â^'xMgxTaO4â^'x/2 ceramics via anion sublattice adjustment. Rare Metals, 2020, 39, 545-554.	3.6	22
21	Effect of atmosphere composition on the oxidation behavior of MCrAlY coatings. Materials and Corrosion - Werkstoffe Und Korrosion, 2011, 62, 699-705.	0.8	21
22	Effect of water vapour on morphology of the Si/Ti-rich phase at the interface between oxide layer and aluminide coating. Corrosion Science, 2020, 163, 108240.	3.0	20
23	A Highly Stable Photodetector Based on a Lead-Free Double Perovskite Operating at Different Temperatures. Journal of Physical Chemistry Letters, 2021, 12, 5682-5688.	2.1	20
24	Influence of water vapour on the HfO2 distribution within the oxide layer on CoNiCrAlHf alloys. Journal of Alloys and Compounds, 2018, 739, 690-699.	2.8	19
25	Enhanced interface adhesion by in-situ oxidation within metal-ceramic coatings. Ceramics International, 2018, 44, 23273-23278.	2.3	19
26	Synthesis, crystal structure and thermophysical properties of (La1-XEuX)3TaO7 ceramics. Ceramics International, 2018, 44, 16273-16281.	2.3	19
27	Diffusion characteristics and structural stability of Pt modified β-NiAl/γ′-Ni3Al within NiCoCrAl alloy at high temperature. Applied Surface Science, 2019, 476, 1096-1107.	3.1	18
28	Synthesis and thermophysics properties of ferroelastic SmNb1-XTaXO4 ceramics. Ceramics International, 2018, 44, 13999-14006.	2.3	17
29	Oxidation properties and microstructure of a chromium coating on zircaloy-4 fuel cladding material applied by atmospheric plasma spraying. Journal of Nuclear Materials, 2022, 560, 153496.	1.3	17
30	Non-isothermal crystallization kinetics of a Fe–Cr–Mo–B–C amorphous powder. Journal of Alloys and Compounds, 2020, 823, 153783.	2.8	16
31	Influence of heat treatment on alternant-layer structure and mechanical properties of Al2O3-TiO2-MgO coatings. Ceramics International, 2018, 44, 13727-13735.	2.3	15
32	Heat-induced interface-coupling behaviour of thermally sprayed Cu/ceramic coatings. Ceramics International, 2018, 44, 11918-11922.	2.3	15
33	Fabrication and characterization of 8YSZ ceramic based abradable seal coatings by atmospheric plasma spraying. Ceramics International, 2020, 46, 26530-26538.	2.3	15
34	Improvement in the mechanical properties of plasma spray ceramic-Cu/TI3AlC2 gradient coatings by heat treatment. Ceramics International, 2019, 45, 22452-22463.	2.3	14
35	Tribological performance and phase transition of MAX-phase/YSZ abradable seal coating produced by air plasma spraying. Ceramics International, 2022, 48, 4188-4199.	2.3	14
36	Influence of zirconia alloying on the thermophysical and mechanical properties of YTaO4 ceramics. Ceramics International, 2019, 45, 24894-24899.	2.3	13

#	Article	IF	CITATIONS
37	Influence of microstructure on hardness of plasma sprayed Al ₂ 0 ₃ –TiO ₂ –MgO coatings with interface diffusion by heat treatment. Materials Research Express, 2017, 4, 126402.	0.8	12
38	Thermophysical properties of rare earth barium aluminates. Journal of the American Ceramic Society, 2018, 101, 2718-2723.	1.9	12
39	Analysis of structure and microhardness of Al2O3-40 wt.% TiO2/NiCoCrAl gradient coating with in-situ needle-like phase reinforcement after high-temperature treatment. Ceramics International, 2019, 45, 14546-14554.	2.3	12
40	Thermophysical and mechanical properties of YTaO4 ceramic by niobium substitution tantalum. Materials Letters, 2020, 268, 127586.	1.3	12
41	Effect of the interface morphology and initial nanocrack on the fracture property of a ceramic reinforced plasma-sprayed coating. Ceramics International, 2020, 46, 24930-24939.	2.3	12
42	Effect of Pt doping on oxide scale formation on yttria-dispersion FeCrAl alloy at 1200â,, <i>f</i> . Corrosion Science, 2020, 168, 108580.	3.0	12
43	Potential thermal barrier coating materials: RE2FeTaO7 (REÂ= Y, Eu, Gd, Dy) compounds. Journal of Alloys and Compounds, 2021, 855, 157408.	2.8	12
44	CrO2(OH)2 volatilization rate and oxidation behavior prediction of the NiCr coating in air-H2O environment at 650 $\hat{a}_{,,f}$. Corrosion Science, 2021, 182, 109303.	3.0	12
45	Enhanced thermoelectric properties of Pb-doped Cu1.8S polycrystalline materials. Solid State Sciences, 2019, 95, 105953.	1.5	10
46	Effect of water vapor on the failure behavior of thermal barrier coating with Hf-doped NiCoCrAlY bond coating. Journal of Materials Research, 2019, 34, 2653-2663.	1.2	10
47	Test atmospheres affecting voids distribution on MCrAlY-bond coats for TBCs at 1050°C. Corrosion Science, 2022, 195, 109967.	3.0	10
48	Effect of O2 on reduction of NO2 with CH4 over gallium-modified ZnAl2O4 spinel-oxide catalyst by first principle analysis. Applied Surface Science, 2015, 349, 138-146.	3.1	9
49	Phase transition and interface evolution of Al2O3/ZrO2 particles in plasma-sprayed coatings. Ceramics International, 2020, 46, 12275-12281.	2.3	9
50	Evolution of in-situ pores and high-temperature thermal-barrier performance of Al-Si coating on NiCoCrAl alloy. Surface and Coatings Technology, 2018, 344, 489-498.	2.2	8
51	Effect of in-situ oxidation on the nanomechanical evolution of Fe-base coating with ceramic particles produced by internal rotating plasma spraying. Ceramics International, 2019, 45, 19856-19863.	2.3	8
52	Effect of partial crystallization of an amorphous layer on the mechanical properties of ceramic/metal-glass coating by thermal spraying. Ceramics International, 2019, 45, 18803-18813.	2.3	8
53	Thermophysical properties of Yb(Ta Nb1â^')O4 ceramics with different crystal structures. Ceramics International, 2020, 46, 28451-28458.	2.3	8
54	First-principles calculations of NO and NO2adsorption on a spinel ZnGaAlO4(100) surface. Physica Scripta, 2014, 89, 075401.	1.2	7

#	Article	IF	CITATIONS
55	Surface texture of substrates prepared by femtosecond laser for improving the thermal cycle life of TBCs. Ceramics International, 2022, 48, 5775-5786.	2.3	7
56	Destructive Effect of Water Vapour on an In Situ Diffusion Barrier Layer within an Aluminide Coating on IN738 Alloy. Coatings, 2018, 8, 332.	1.2	6
57	Microstructure and interface-adhesion of thermally sprayed continuous gradient elastic modulus FeCrAl-ceramic coatings. Ceramics International, 2020, 46, 5946-5959.	2.3	6
58	Nanoindentation creep behavior of an Fe–Cr–Mo–B–C amorphous coating via atmospheric plasma spraying. Intermetallics, 2022, 141, 107411.	1.8	6
59	Effect of water vapor on evolution of a thick Pt-layer modified oxide on the NiCoCrAl alloy at high temperature. Materials Research Express, 2018, 5, 036514.	0.8	5
60	Effect of YSZ-dopant on microstructure and hardness property of the Al ₂ O ₃ –40%TiO ₂ plasma sprayed coating. Materials Research Express, 2018, 5, 086504.	0.8	5
61	Fabrication and characterization of Ni-decorated h-BN powders with ChCl-EG ionic liquid as addition by electroless deposition. Royal Society Open Science, 2018, 5, 180146.	1.1	5
62	High temperature mechanical and thermal properties of CaxBa1-xZrO3 solid solutions. Ceramics International, 2020, 46, 17416-17422.	2.3	5
63	Effect of water vapor on the oxide growth in FeCrAl-based oxide dispersion-strengthened fuel cladding material at 1100Ââ,, f and 1200Ââ,, f. Corrosion Science, 2021, 191, 109775.	3.0	5
64	Effect of external pressure on <i>î²</i> -NiAl phase transformation of Co-base alloy at 1323 K. Materials Research Express, 2019, 6, 1265b2.	0.8	4
65	Investigation of oxide scale formation and internal oxidation of an Fe-based coating at 500°C and 600°C. Surface and Coatings Technology, 2020, 402, 126309.	2.2	4
66	Microstructure and thermophysical properties of CeO2-doped SmTaO4 ceramics for thermal barrier coatings. Journal of Materials Research, 2020, 35, 242-251.	1.2	4
67	Effect of platinum and pre-oxidation on the hot corrosion behavior of aluminide coating with NaCl at 1050 °C. Materials Research Express, 2020, 7, 116402.	0.8	4
68	The effect of bulk conversion into surface on physical properties of HfO2: First principle study. Materials Science in Semiconductor Processing, 2022, 146, 106650.	1.9	4
69	Effect of Thermal Cycling on Lifetime and Failure Mechanism of EB-PVD TBC with NiCoCrAlYZr Bondcoats. Advanced Materials Research, 0, 652-654, 1826-1829.	0.3	3
70	Cyclic oxidation behaviour of Pt-doped aluminide coating on DZ125 containing Hf. Materials Research Express, 2019, 6, 126536.	0.8	3
71	First-principle-based structural and thermodynamic parameters of Ni–Al intermetallic compounds under different pressures and temperatures. Modern Physics Letters B, 2021, 35, 2150124.	1.0	3
72	Influence of Gradient Index and Pores on the Properties and Internal Stress of Continuous Transition Ceramic–Metal Coating. Coatings, 2022, 12, 569.	1.2	3

#	Article	IF	CITATIONS
73	Interdiffusion Behaviour of Silicon-Modified Aluminide Coating in Atmospheres Containing Water Vapour at 1050°C. Oxidation of Metals, 2022, 98, 179-198.	1.0	3
74	The thermophysical properties and defect chemistry of HfO2–Sm3TaO7 ceramics. Journal of Materials Research, 2020, 35, 2230-2238.	1.2	2
75	Irradiation with phosphorus ions modifies the structure and tunable band-gap of a hexagonal AlN thin film. Applied Physics A: Materials Science and Processing, 2021, 127, 1.	1.1	2
76	Non-isothermal crystallisation behaviour of a Cr–Fe–Ni–Co–Mo–Si amorphous coating. Materials Today Communications, 2022, 30, 103094.	0.9	2
77	Effect of Polishing Treatment on Rumpling of Oxide Scales on NiPtAl Coatings with Different Pt-Content. Advanced Materials Research, 2013, 662, 383-386.	0.3	1
78	Influence of Impact Damage on the Thermal Stress Distribution within the EB-PVD Thermal Barrier Coatings. Materials Science Forum, 0, 849, 683-688.	0.3	1
79	Effect of the Porosity on Thermal Stress within TBCs Using Finite Element Method. Materials Science Forum, 2016, 849, 689-694.	0.3	1
80	Alumina Growth and Interface Strengthening Mechanisms of Pt on the Surface of Bond Coats in EB-PVD TBC System Based on First-Principles. Materials Science Forum, 2016, 850, 253-258.	0.3	1
81	Influence of Pre-Oxidation on High Temperature Oxidation and Corrosion Behavior of Ni-Based Aluminide Coating in Na2SO4 Salt at 1050°C. Frontiers in Materials, 2021, 8, .	1.2	1
82	The growth mechanism of oxide scale with Pt on NiCoCrAlY coating in water vapor at 1050â~C. Modern Physics Letters B, 2021, 35, 2150111.	1.0	1
83	Effect of pre-oxidation treatment on the hot corrosion behavior of pack-cemented aluminide coatings on the K438 alloy in salt mixture. Corrosion Communications, 2022, 5, 1-13.	2.7	1
84	Effects of Stepped Heating on the Initial Growth of Oxide Scales on NiCrAlHf Bond Coat Alloy under Air and Water Vapor Atmospheres. Materials, 2022, 15, 2914.	1.3	1
85	Effect of Water Vapor on the Microstructure of Al2O3 on the Free-Standing MCrAlY Alloy at 1100 °C. Metals, 2022, 12, 865.	1.0	1
86	Effect of Pt Content on TGO Growth in EB-PVD TBC Systems with Niptal Bondcoats. Advanced Materials Research, 0, 690-693, 2051-2054.	0.3	0
87	Effect of Atmosphere Composition on Lifetime and Oxidation Behavior of EB-PVD TBC with NiPtAl Bondcoats. Advanced Materials Research, 0, 652-654, 1822-1825.	0.3	0
88	Solid solution mechanism and thermophysical properties of HfO2-SmTaO4 ceramics. Materials Today Communications, 2021, 26, 101927.	0.9	0
89	Difference oxidation behaviors of Ni8Al and Ni25Cr coatings in air with water vapor at 650â ^{~~} . Modern Physics Letters B, 0, , 2150274.	1.0	0
90	Beneficial effects of flame pre-oxidation on the oxidation behavior of NiCoCrAlHf alloy at 1050â,,f. Journal of Materials Research, 0, , .	1.2	0